III. GROWTH ON OFF ORIENTED SUBSTRATES

1. Introduction

In this chapter, some attempts to improve grown layers on Si(100) and (111) by the introduction of off orientation are mentioned.

The main interest in the grown layers on (100) is concerned with antiphase domains(APD's). APD's are crystal defects which are observed in compound crystals. Especially, they are often observed in a heteroepitaxially grown crystal with a zinc-blende structure on a (100) face of a crystal with a diamond structure[1-5]. In the case of a zinc blende crystal like 3C-SiC, APD's are defined as follows. Zinc-blende structures consist of two sublattices of a face centered cubic structure. Usually each sublattice consists of atoms of a kind. When these atoms belong to the opposite sublattice in the both sides of some boundaries, the boundaries are called antiphase boundaries(APB's). Domain structures made by APB's are called APD's. A model of APD's(APB's) in a zinc blende structure is shown in Fig.1. In a zinc-blende structure each atom has four bondings with the nearest atoms of the opposite kind. However, APB's consist of bondings with atoms of the same kind as shown in Fig.1. When a crystal containing APD's is observed from [100], [011] direction in one domain is 90° different from that in a adjoining domain separated by APB's. In other words, when grown layers on Si(100) are observed from the upper side, it looks that there are two phases which are rotated by 90° each other.

APB's in semiconductor materials should be eliminated. In the case of epitaxial layers of GaAs on Si, APB's work as origins of lowering of electron mobility[6], roughness of surfaces[6] and recombination centers[7]. In this chapter, the origin and how to eliminate APD's in 3C-SiC are discussed based on various observations. Electrical properties are mentioned in the next chapter.

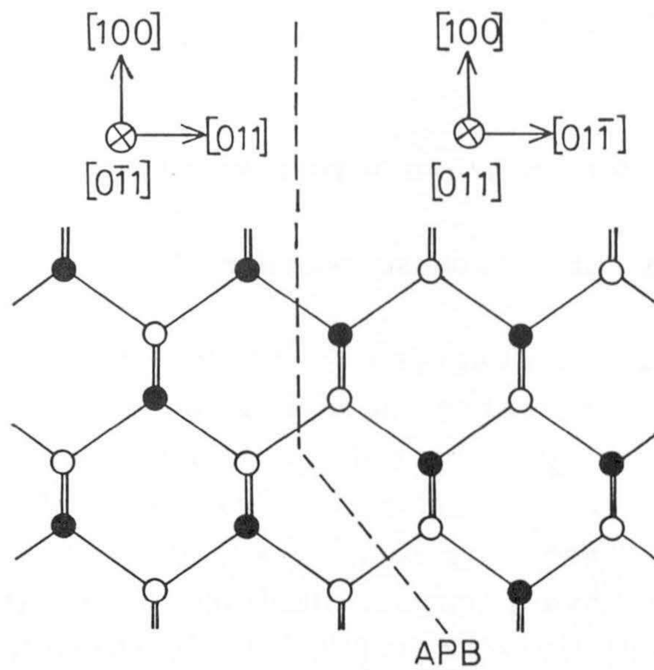

Fig.1 Antiphase boundary in a zinc blende crystal.

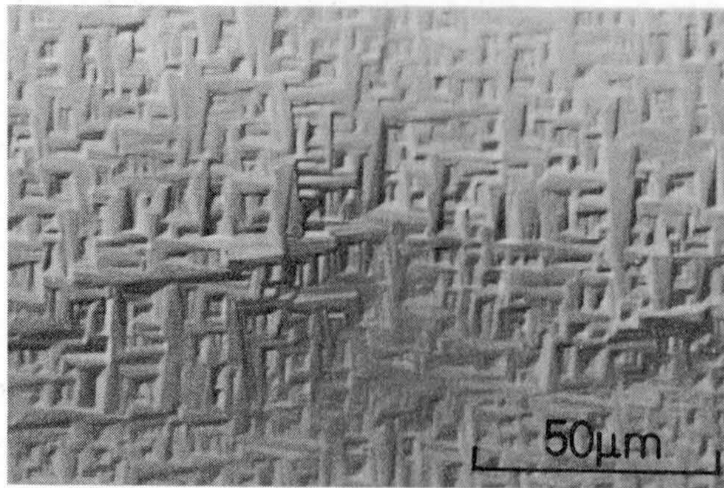

Fig.2 Nomarski microphotograph of typical surface morphology of the grown layer on a (100) well oriented substrate.

In Section 4, a fundamental experiment to investigate effects of the introduction of off orientation into (111) substrates is mentioned.

2. Antiphase disorder in grown layers on Si(100)

2-1. Observation of antiphase boundaries

APD's were always observed in 3C-SiC grown layers on (100) well oriented Si substrates. Figure 2 shows a typical surface morphology of grown layers on (100) well oriented substrates. The observed texture-like morphology consists of wedge shapes perpendicularly intersecting each other. Here, the existence of two phases which have perpendicular relationships should be noted. As explained above, two phases separated by APB's show a perpendicular relationship. Therefore, the surface morphology in Fig.2 is considered to indicate the existence of APD's. Such morphology was reported in the case of GaP grown layers on Si(100) which contained APD's.[1].

The existence of APD's in grown layers on (100) well oriented substrates was inferred by the surface morphology. By utilizing other techniques the existence of APD's was confirmed clearly. In this section etching and B-doping methods are mentioned. APB's were visualized using these methods. The utilization of a RHEED technique for the identification of the existence of APD's is mentioned in Section 2-3.

First, an etching method for the observation of APB's is introduced. Molten-alkali etching is known to be a good defect-observation tool for (0001)Si faces of various polytypes of SiC[8]. However, no one reported whether molten-alkali etching is useful for the 3C-SiC(100) face or not as far as the author knows. In this investigation it was confirmed that defects were observed by molten KOH etching as hollows on the SiC(100) surface. Figure 3 shows an etched surface by molten KOH at about 600°C. Three types of hollows were observed : A:type-1

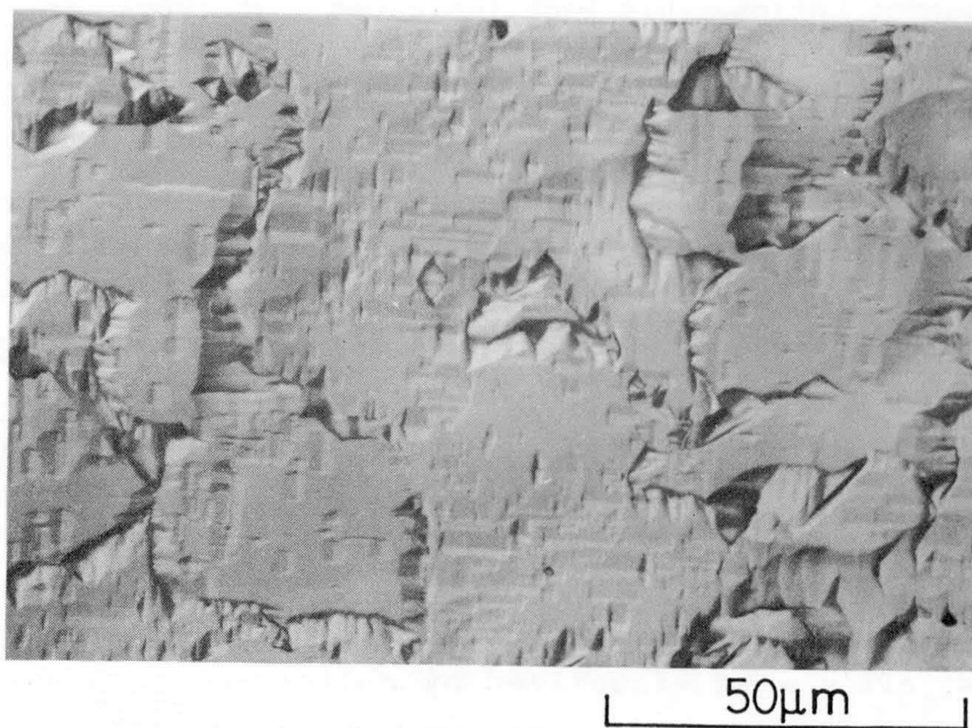

Fig.3 Nomarski microphotograph of the surface of a grown layer etched by molten KOH on (100) well-oriented substrate. APB's were observed as random grooves.

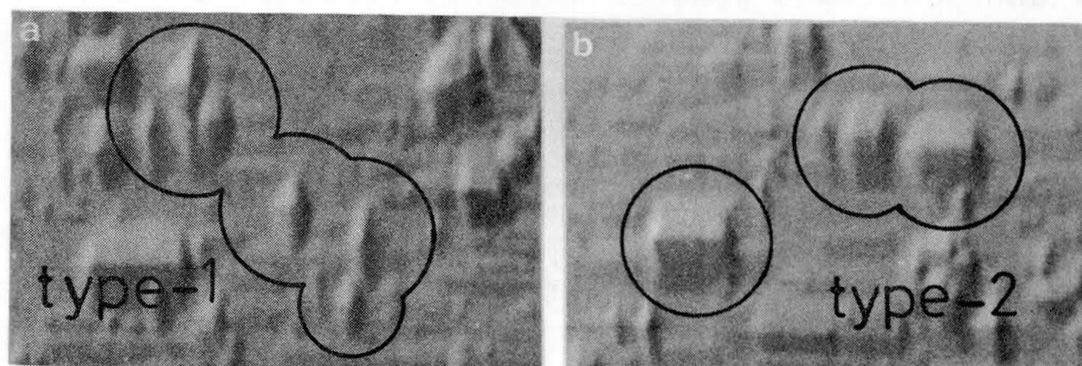

Fig.4 Etch pits formed by molten KOH etching. (a)type-1 pits and (b)type-2 pits.

pits(Fig.4(a)), B:type-2 pits(Fig.4(b)) and C:random grooves. Every type-1 pit has a similar figure and type-2 pits have various aspect ratios. This fact indicates that type-1 and 2 pits originate from line defects(dislocation) and plane defects(stacking faults), respectively. Random grooves are visualized APB's, because the pits are placed perpendicularly each other in adjoining regions separated by the grooves.

Figures 5(a)-(c) show Nomarski microphotographs of etched surfaces of grown layers with various thicknesses. APD's became broader and the concentration of APB's was reduced as a film grew thicker. Figures 6(a)-(c) indicate a reduction mechanism of APB's. As the film becomes thicker, APB's spread upward with lateral movements(Figs.6(a) and (b)). And once two APB's collide, they connect each other and stop spreading(Fig.6(c)). Thus, APB's reduce and the area of a single domain becomes broader, as the film grows.

Thus, APB's were visualized by molten KOH etching. APB's could be also observed by B-doping during CVD growth. A B-doped layer was grown after etching by HCl at 1330°C on an undoped grown layer of 10μm thick. The thickness of the B-doped layer was about 1μm. APB's were clearly observed as grooves as shown in Fig.7. However, the area where grooves were formed was very narrow and sometimes grooves were not formed. Therefore, the molten KOH etching method was mainly used for the identification of the elimination of APD's.

2-2. Elimination of antiphase boundaries

Kroemer et al. indicated two necessary conditions to obtain an APD-free grown layer with a zinc-blende structure on the (100) face of a substrate with a diamond structure[2]. The conditions are the followings.

(A): There is a chemical preference for A-S bonding over B-S bonding. Where A and B are elements which constitute the zinc blende grown layer and S is an element of the substrate.

(B): The substrate should not have steps with a mono(or odd

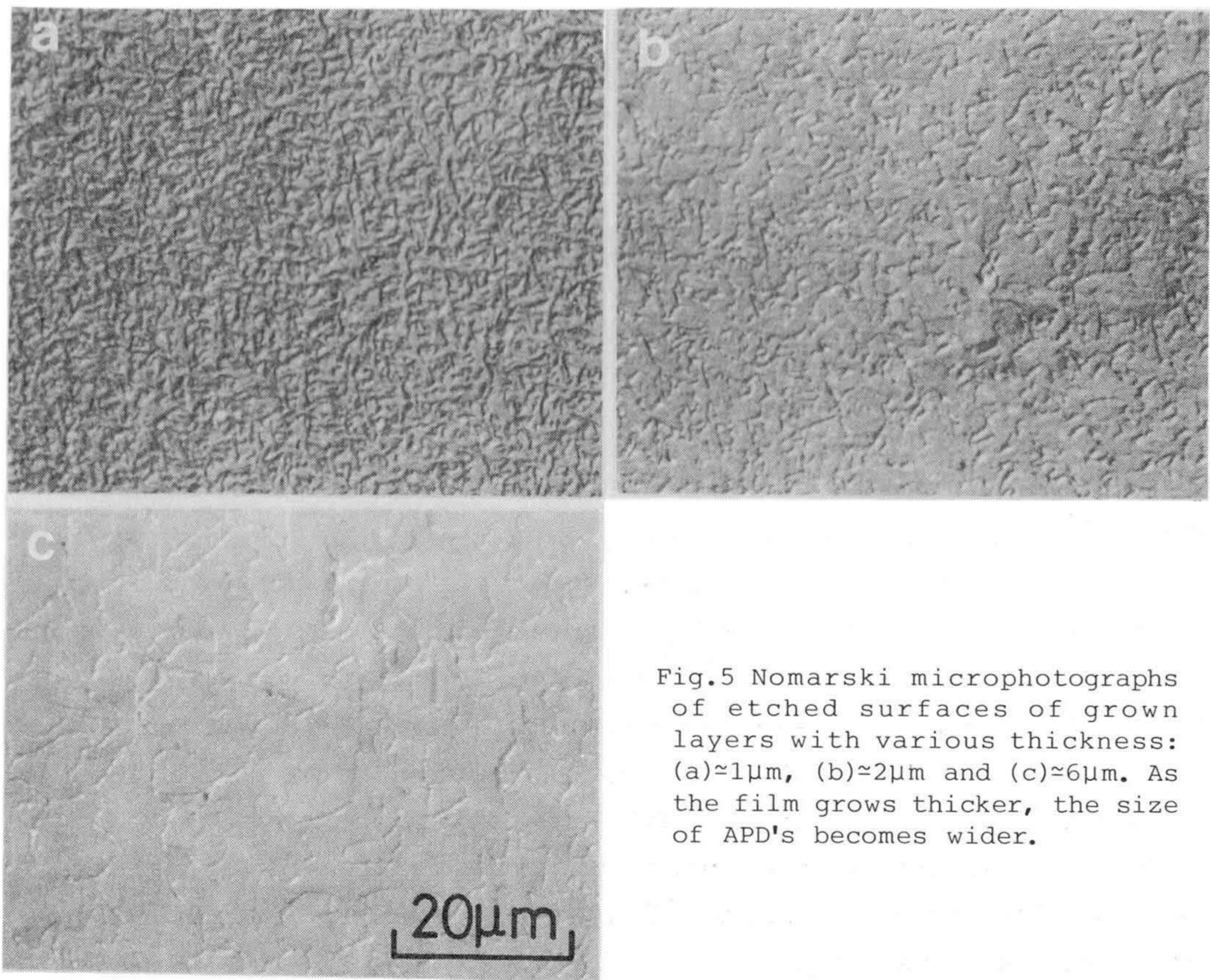

Fig.5 Nomarski microphotographs of etched surfaces of grown layers with various thickness: (a)≃1μm, (b)≃2μm and (c)≃6μm. As the film grows thicker, the size of APD's becomes wider.

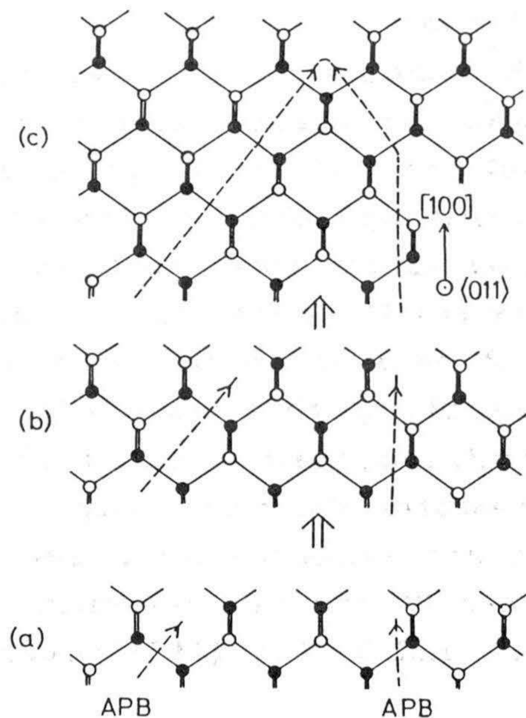

Fig.6 Model of the reduction mechanism of APB's. The crystal is viewed in the <011> direction.

number)-atomic layer height.

The condition (A) means that the first grown layer must consist of atoms of one kind. As discussed in Chapter II, the first grown layer formed by the carbonization of Si was considered to consist of C atoms only. So that, the condition (A) is satisfied. Hence, if the surface where only steps with a bi(or even numbers)- atomic layer height is obtained, an APD-free growth is expected as shown in Fig.8(a). However, APD's actually existed in the grown layer. Steps with a mono-atomic layer height which existed on the surfaces of etched Si substrates by HCl were considered to be origins of APB's as shown in Fig.8(b). Some methods to obtain a Si surface with bi-atomic layer steps are necessary for an APD-free growth. Modification of the step height on Si(100) under an ultra high vacuum was observed by LEED and RHEED[9-11]. The introduction of off orientation into Si(100) or surface treatment at high temperatures were effective to obtain bi-atomic layer steps. In this investigation, the elimination of APD's by the introduction of off orientation was attempted.

The off orientation consists of two important factors of the direction and the magnitude of an off angle. In order to treat these two factors at the same time, 3C-SiC was grown on a spherically polished Si(100) substrate. The radius of the curvature of the spherically polished substrate was 14cm. Figure 9(a) shows a photograph of the surface of the grown layer on the spherically polished substrate. Two black crossing lines were observed. These lines crossed at the (100) pole, and spread towards the directions which are equivalent to the [011] direction. The surface on the two black lines was mirrorlike, and that on the other area was rough. Figures 10(a)-(d) show Nomarski microphotographs of the surfaces at various points which are indicated in Fig.9(b). Point A corresponds to the (100) pole. In other words, the grown layer on point A corresponds to that on the (100) well-oriented surface. A texture-like morphology which indicates the existence of APD's was observed as shown in Fig.10(a). The grown layers on points B1 and B2 correspond to those on the surfaces oriented 1° and 3° off (100) towards

Fig.7 SEM microphotograph of the visualized APB's by the growth of a B-doped layer.

Fig.8 Model of origin of APD. On the assumption that the first grown layer consists of C atoms only, (a)steps with bi-atomic layer height result in APD-free growth. (b) Steps with mono-atomic layer height result in formation of APB's.

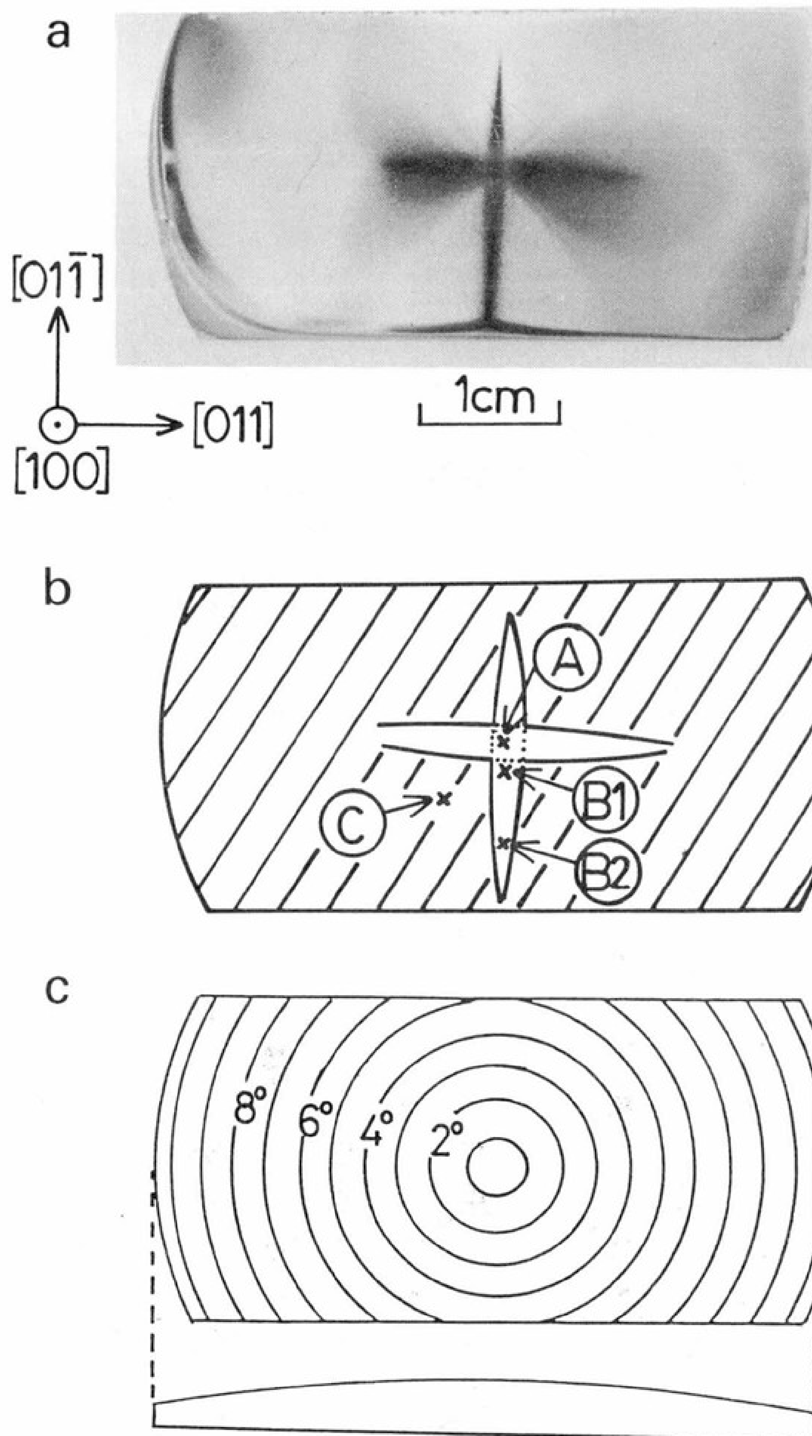

Fig.9 (a)Photograph of a grown layer on a spherically polished (100) substrate. The rough surface area looked white or grey because of random reflection of lighting. The surface of two black lines was mirrorlike. (b)Positions of points *A*, *B1*, *B2* and *C* on the spherically polished substrate. The surface morphology of the grown layers on these points is shown in Fig.10. The surface of the unshaded area was mirrorlike and that on the shaded area was rough. (c)Schematic explanation of relationship between position and off angle.

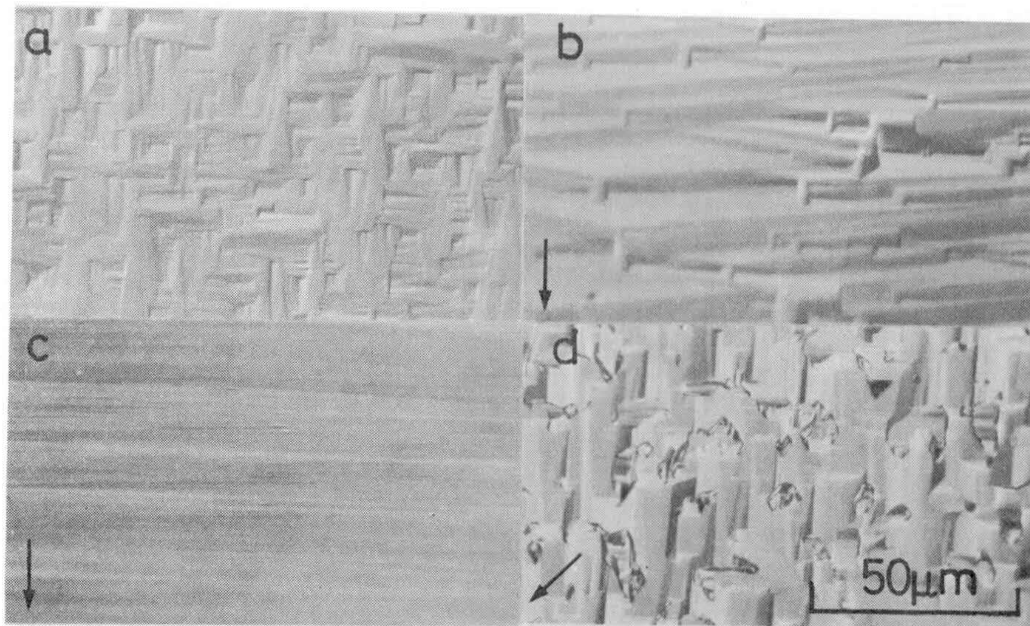

Fig.10 Nomarski microphotographs of the surfaces at various points of the grown layer on the spherically polished (100) substrates. Points *A*, *B1*, *B2* and *C* are located at (a)(100) pole, (b)the point inclined at 1° towards (011), (c)the point inclined at 3° towards (011) and (d) the point inclined at 4° towards (010).

(011), respectively. From point A to point B2 the surface morphology changed gradually. As the magnitude of the off angle became larger, the wedge-like crystal habit which pointed the perpendicular direction to the off direction became dominant like in Fig.10(b). Even when the magnitude of the off angle reached to 1°, antiphase domains were still observed like small islands(Fig.10(b)). Beyond 2° of the magnitude of the off angle, antiphase domains were not observed as shown in Fig.10(C). Up to 5° the single-domain area was observed. Beyond 5° the existence of antiphase domains was not clear because of surface roughness which was brought about by the disturbance of gas flow due to the thick and curved substrate. Off orientations except for towards [011] resulted in very rough surfaces with APD's like on point C(Fig.10(d)).

These results were applied to the growth on Si(100) wafers. The substrates used were oriented 2° off (100) towards (011). The surface morphology was similar to Fig.10(c). In order to confirm the elimination of APD's, the grown layer was etched with molten KOH at about 600°C. As shown in Fig.11, the etched surface of the grown layer on the substrate oriented 2° off (100) towards (011) showed no grooves, and all etch pits have the same direction different from the grown layers containing APD's. This result means that APD's were eliminated by the introduction of the off orientation towards (011). Substrates oriented 4° and 6° off (100) towards (011) were also used. The surface morphology for these substrates was quite similar to that for 2° off.

Figure 12 explains the relationship between the off orientation and surface morphology or etch pits. This relationship was constant. By using this, a strict epitaxial relationship between off substrates and grown layers is discussed as follows. The top view of type-2 pits is rhombic. In 6H-SiC, the $(000\bar{1})$C face is chemically more active than the (0001)Si face, and the former has a higher etch rate for molten alkali. The $(000\bar{1})$ and (0001) faces correspond to the $(11\bar{1})$ and (111) faces of 3C-SiC, respectively. If the sidewalls of the etch pits consist of only the $(11\bar{1})$ and (111) faces, the longer

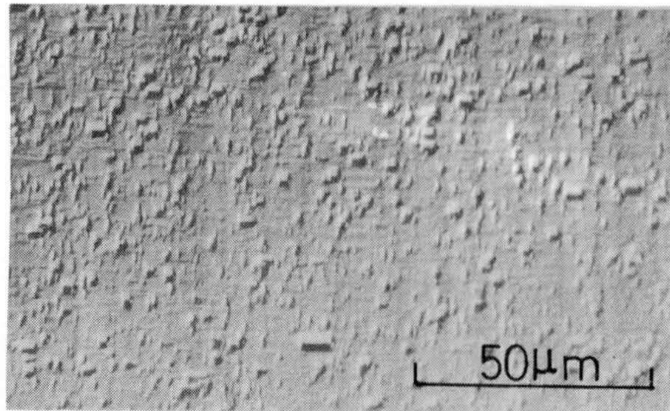

Fig.11 The surface of the grown layer etched with molten KOH on a Si substrate oriented 2° off (100) towards (011). No APB's are observed.

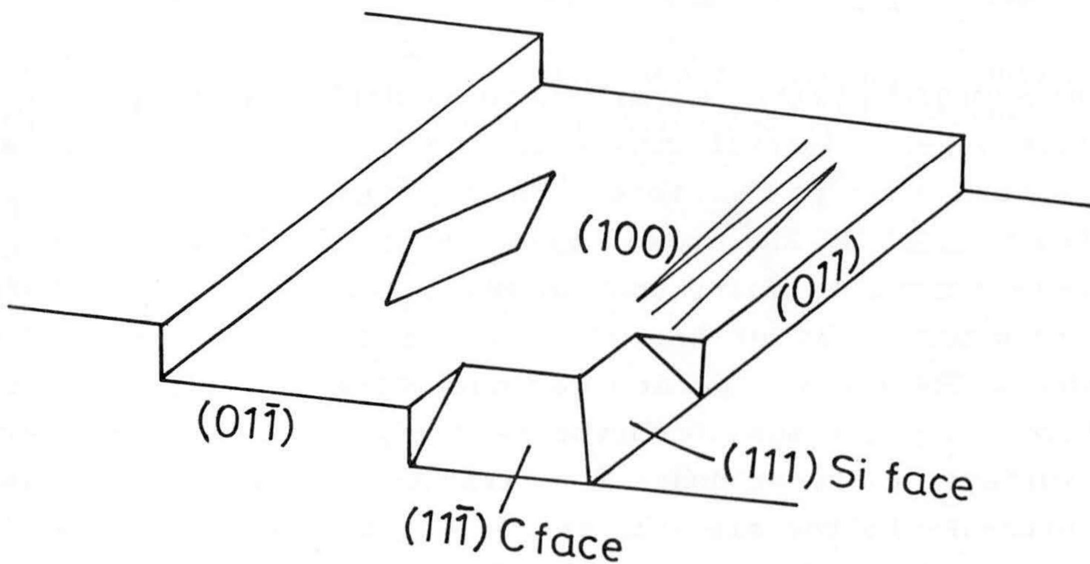

Fig.12 Schematic explanation of the relationship between off direction and etch pits or wedge-shaped surface morphology.

diagonal line of the rhombic shape should point the direction of the higher etch rate as shown in Fig.13. Therefore, the relationship between the off orientation and the $(11\bar{1})$ or (111) faces are obtained as shown in Fig.12.

An example of the surface morphology of the grown layers on Si oriented 4° off (100) towards (010) is shown in Fig.14. The surface was rough and the existence of APD's was confirmed by molten KOH etching. Thus, the grown layers on spherically polished (100) substrates and various (100) wafers well agreed concerning the existence of APD's and surface morphology.

In this investigation, the off orientation was introduced to eliminate APD's. Recently this method is often used for the growth of III-V semiconductors on Si[3,12,13]. Growth on Si(211) is also known as a method to obtain APD-free grown layers for GaP and GaAs[14,15]. However, this method cannot be adopted for 3C-SiC, because single crystals could not be grown on Si(211) as mentioned in Section II-5.

2-3. Surface observation by RHEED

In Section 2-1 the observation of APB's was described. In this section, the identification of the existence of APD's using a RHEED technique is mentioned. This method utilizes a surface 5x1 structure of 3C-SiC grown layers. This surface structure was very persistent. In spite that samples were exposed to the air for a long period after growth, the surface structure did not disappear. The longest period was over several months. Surface structures of other semiconductor materials are usually observed after surface treatment under an ultrahigh vacuum and they vanish after exposure to the air[16]. The 5x1 structure was observed as the fifth order extra streaks in RHEED patterns. In addition that, curved streaks due to reciprocal planes were observed. The relationship between the 5x1 surface structure and the curved streaks is also discussed.

Two types of Si substrates were used. One was a (100) well oriented Si substrate and the other was a Si substrate oriented

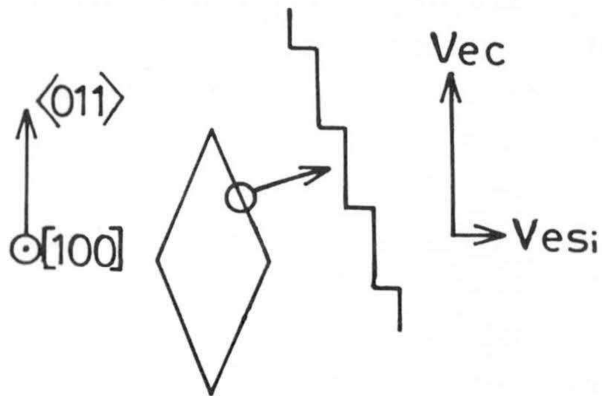

Fig.13 If the sidewall of etch pits consists of only $(11\bar{1})$C and (111)Si faces, a longer diagonal line of rhombic shape points $[11\bar{1}]$ direction because of the difference in etch rates.

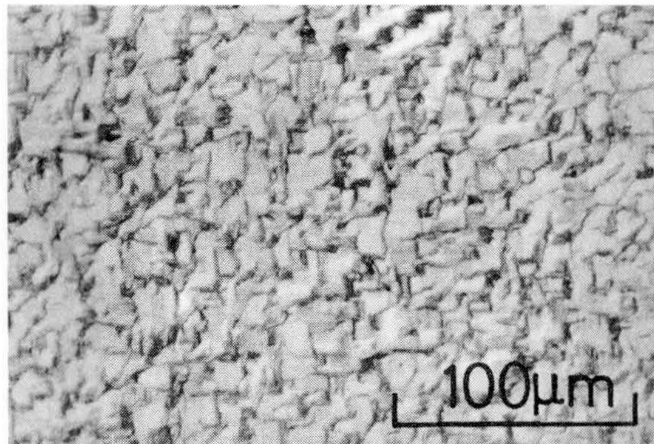

Fig.14 Nomarski microphotograph of surface morphology of a grown layer on Si substrates oriented 4° off (100) towards (010).

2° off (100) towards (011). The former and the latter substrates are hereafter called as (100) substrates and off substrates in this section, respectively. The grown layers on (100) substrates contained APD's as described in Section 2-1.

RHEED observations were carried out using a JEOL JEM-120B electron microscope with an attachment for high resolution RHEED. The acceleration voltage of incident electrons was 80kV. Samples were left in the air after growth. No surface treatment was carried out in the microscope. Sometimes samples were cleaned with organic solvents, deionized water or HF acid. However, cleaning seemed to give no difference in RHEED patterns. Surface structures were reproducibly observed when the grown layers were thicker than 0.5μm. RHEED patterns used hereafter were taken with the grown layers of 0.5μm in thickness.

Figures 15(a)-(d) show RHEED patterns for the $\langle 011 \rangle$ azimuth. In the case of the grown layers on (100) substrates(Figs.15(a) and (b)), both $[0\bar{1}1]$ and [011] azimuth patterns showed the fifth order extra streaks. The pattern was schematically represented in Fig.16. In the [001] azimuth no extra streaks were observed as shown in Fig.17(a). Hence, these RHEED patterns originated from a mixture of the 5x1 and 1x5 surface structures; i.e. two phases existed on the surface of the grown layer on the (100) substrates. The grown layers on the (100) substrates contained APD's. If these two phases originated from APD's, APD-free grown layers on off substrates should contain a 5x1 structure. The RHEED pattern for the [011] azimuth of the grown layer on the off substrate actually showed no extra streaks as shown in Fig.15(d) and the $[0\bar{1}1]$ azimuth pattern in Fig.15(c) showed the fifth order streaks similar to Figs.15(a) and (b). Thus, CVD grown layers of 3C-SiC on the off substrates showed the 5x1 surface structure. A 6x1 surface structure was rarely observed.

Two kinds of unusual streaks were observed in addition to the fifth order streaks. One is a curved streak and the other is an unusually long streak. The curved streaks were observed in the [010] azimuth patterns of Figs.17(a) and (b). In the case of $\langle 011 \rangle$ azimuth patterns on the off substrates, streaks for

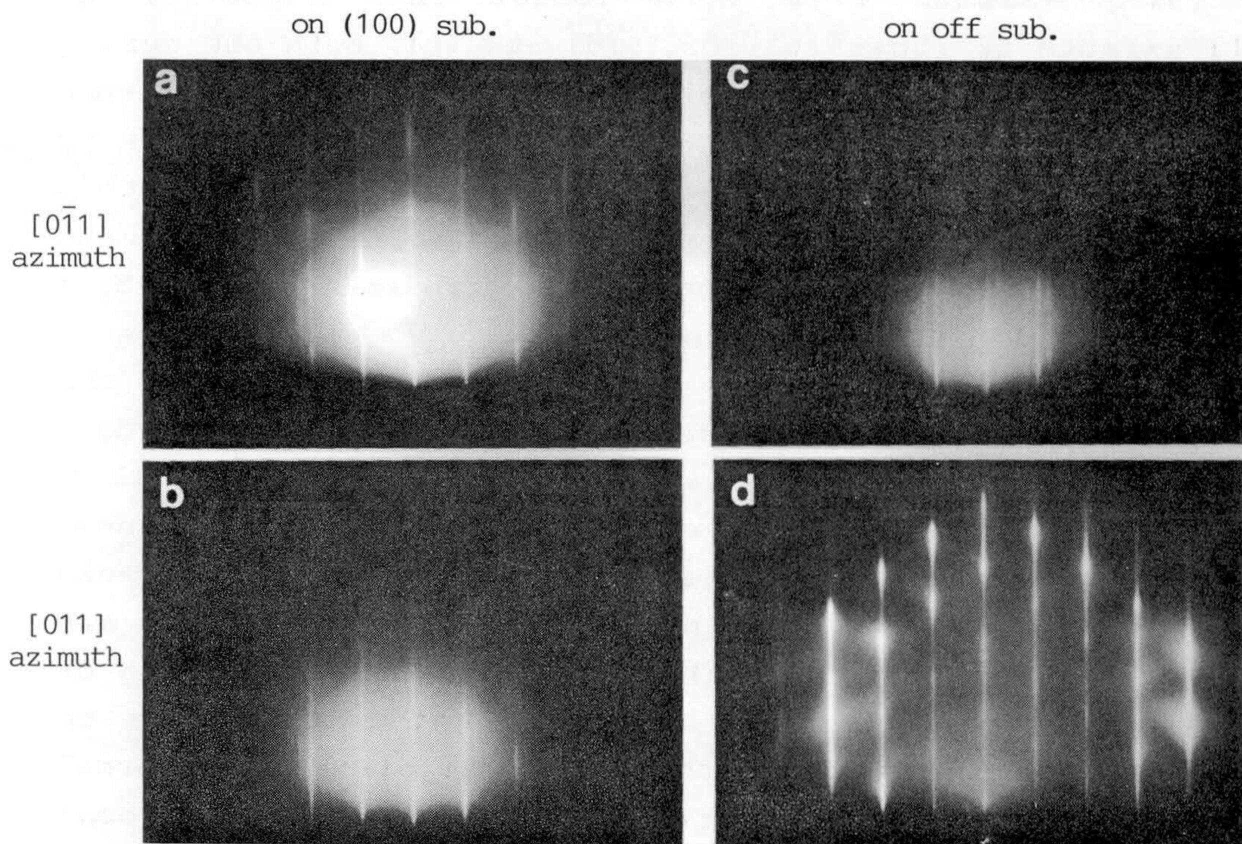

Fig.15 [0$\bar{1}$1] and [011] azimuth RHEED patterns of the grown layers on a (100) substrate and a 2° off substrate.

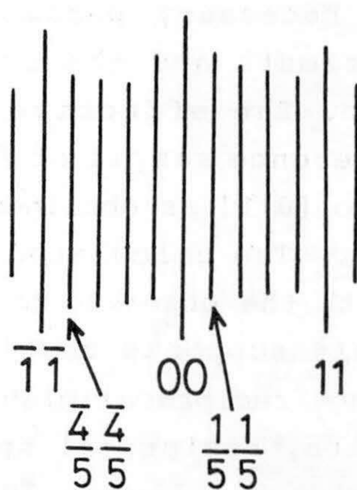

Fig.16 Schematic explanation of Fig.15 (a), (b) and (c).

the [011] azimuth were much longer than those for the $[0\bar{1}1]$ azimuth as shown in Figs.15(d) and (c). Both the curved streaks and unusually long streaks are explained by the existence of reciprocal planes[17-19]. When a structure composed by parallel linear rows exists, the reciprocal lattice of this structure is formed by reciprocal planes normal to the rows. And when the each row consists of components periodically spaced by a distance of d in the real space, the reciprocal planes have an interval of $1/d$ as shown in Fig.18. The projection of the intersectional lines made by the Ewald sphere and the reciprocal planes are observed as the curved streaks on a screen or a film. If the incidence azimuth is parallel to the reciprocal planes, projected intersectional lines are observed as straight streaks as shown in Fig.19(a). If it is not parallel, curved streaks are observed as shown in Fig.19(b). The [011] azimuth pattern of Fig.15(d) showed unusually long straight streaks due to reciprocal planes. Therefore, the reciprocal planes are normal to $[0\bar{1}1]$ direction. The interval of the observed reciprocal planes corresponds to the distance between 00 and $1\bar{1}$ streaks as shown in Fig.15(d), which means that the period of the components composing the each row corresponds to the lattice spacing of (011) faces.

The projected curves can be easily obtained by calculation[18,19]. The necessary parameters are the angle between the incidence azimuth and the reciprocal planes and effective camera length. The effective camera length was determined by using a reference sample of Au. If the reciprocal planes are perpendicular to $[0\bar{1}1]$ as obtained above, the angle is 45° for the [010] azimuth. The calculated curves assuming the angle to be 45° agreed with the observed curves in Fig.17 of the [010] azimuth. This result supports that the observed curved streaks originated from the reciprocal planes normal to $[0\bar{1}1]$.

Based on these results, reciprocal space diagrams of the surface structures were drawn. Figures 20(a) and (b) show the diagrams on the (100) substrates and the off substrates, respectively. Figure 20(a) corresponds to the superposition of

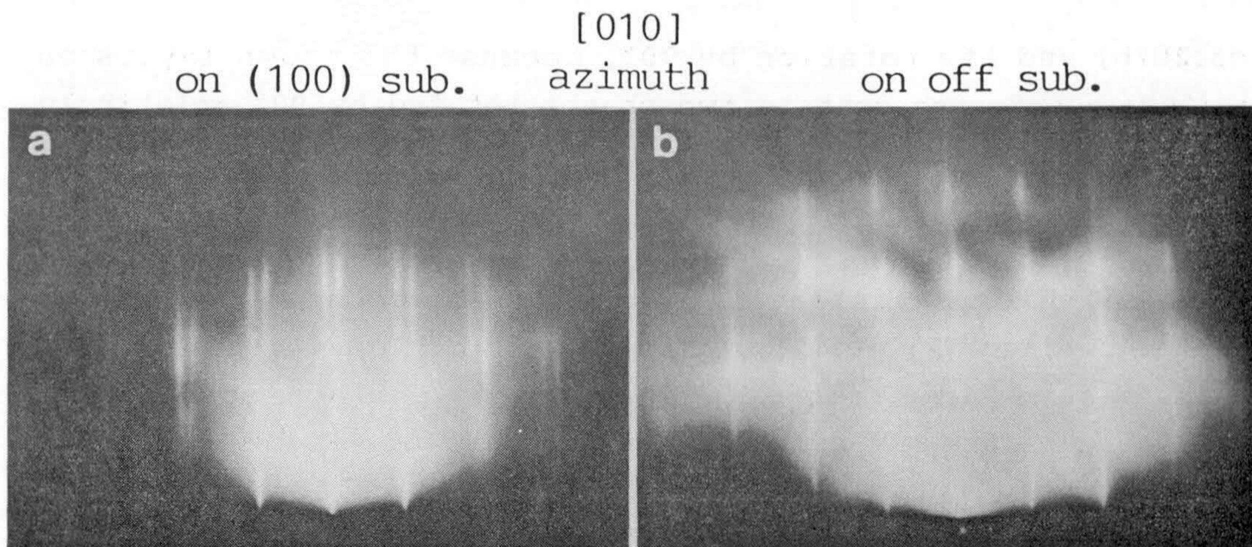

Fig.17 [010] azimuth RHEED patterns of the grown layers (a)on a (100) substrate and (b)on a off substrate.

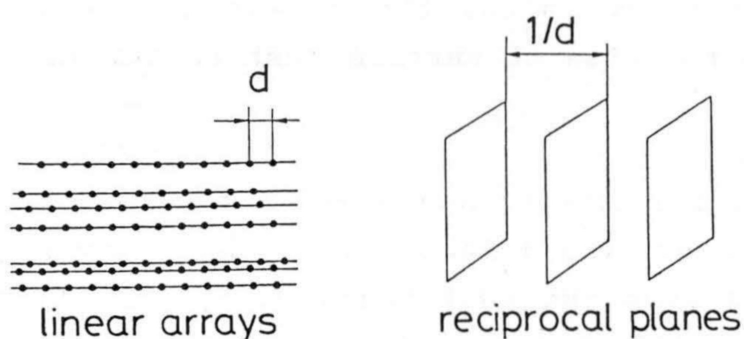

Fig.18 Reciprocal planes are formed in the reciprocal space by linear arrays in the real space. (After Delescluse, Ref.[18]).

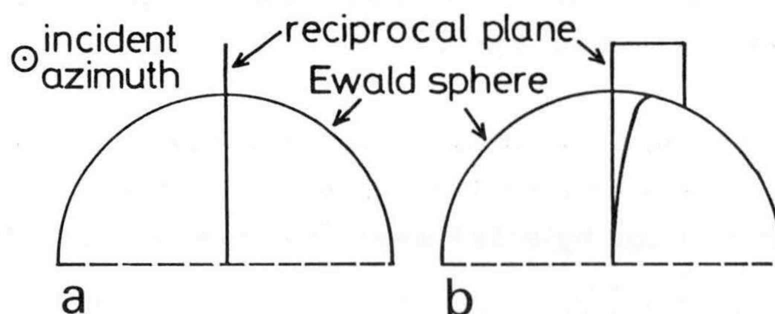

Fig.19 When incident azimuth is (a) parallel and (b) not parallel to a reciprocal plane, intersectional lines made by the Ewald sphere and the reciprocal plane are projected as (a) a straight line and (b) a curved line.

Figs.20(b) and its rotation by 90°, because the grown layers on the (100) substrates contain two phases rotated by 90° relatively due to APD's.

The 5x1 surface structure and the reciprocal planes simultaneously existed as mentioned above. As an example of the structure which satisfies the observed results, a partially occupied surface 5x1 mesh structure shown in Fig.21 is discussed. If the mesh points are fully occupied by surface structures, curved streaks are not observed. In the case of Fig.21, parallel rows are constructed by the missing of surface structures. The rows point the $[0\bar{1}1]$ direction, and each of them is composed by surface structures which lie at intervals of the lattice spacing of (011). A preliminary simulation of diffraction of waves by the 5x1 surface mesh was carried out to discuss the origin of the reciprocal planes. Dynamical theory was not utilized for the simulation. The position of surface mesh points is described as follows:

$$\boldsymbol{R}_m = m_1\boldsymbol{a} + m_2\boldsymbol{b} \ , \qquad (1)$$

where m_1 and m_2 are integer and $\boldsymbol{a}$ and $\boldsymbol{b}$ fundamental translation vectors of the mesh. The difference in the phase angle between scattered waves from the mesh point at $\boldsymbol{R}_m$ and the origin $\boldsymbol{O}$ is written as follows[20]:

$$2\pi(\boldsymbol{s}-\boldsymbol{s}_0)\boldsymbol{R}_m/\lambda = 2\pi\boldsymbol{S}(m_1\boldsymbol{a}+m_2\boldsymbol{b}) \ , \qquad (2)$$

where $\boldsymbol{S}=(\boldsymbol{s}-\boldsymbol{s}_0)/\lambda$, (3)

and $\boldsymbol{s}$ and $\boldsymbol{s}_0$ are wave vectors of incoming and outgoing waves. For the whole mesh points, scattering amplitude F is written as

$$F = \sum_{m_1, m_2} \exp((2\pi i\boldsymbol{S})\cdot(m_1\boldsymbol{a}+m_2\boldsymbol{b})) \ . \qquad (4)$$

Here, since the discussion about the absolute amplitude is not necessary, the scattering factor at mesh points is neglected. To treat the diffraction by a 5x1 mesh, parameters are defined as follows.

$$\boldsymbol{a}=\begin{pmatrix}5\\0\\0\end{pmatrix},\quad \boldsymbol{b}=\begin{pmatrix}0\\1\\0\end{pmatrix},\quad \boldsymbol{s}_0=\begin{pmatrix}0\\0\\1\end{pmatrix},\quad \boldsymbol{s}=\begin{pmatrix}p\\q\\r\end{pmatrix},\quad \lambda=10^{-2} \ . \qquad (5)$$

Then F is described as

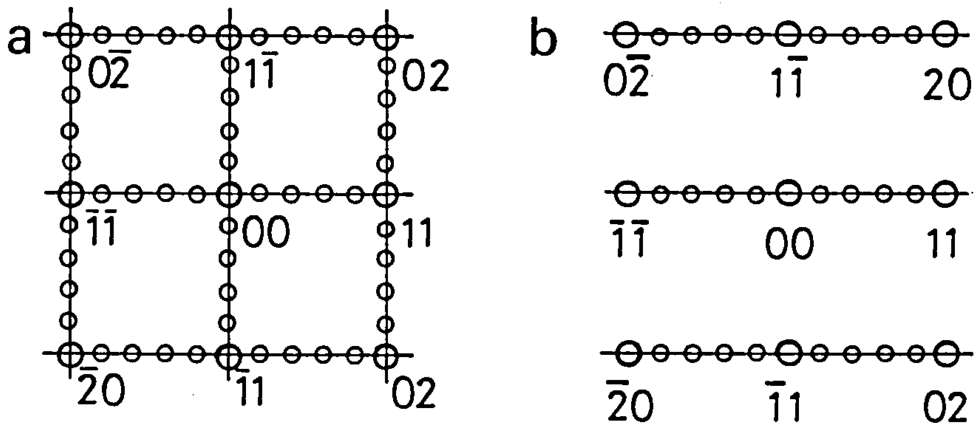

Fig.20 Reciprocal-space diagrams of the surface structure (a)on (100) substrates and (b)on off substrates.

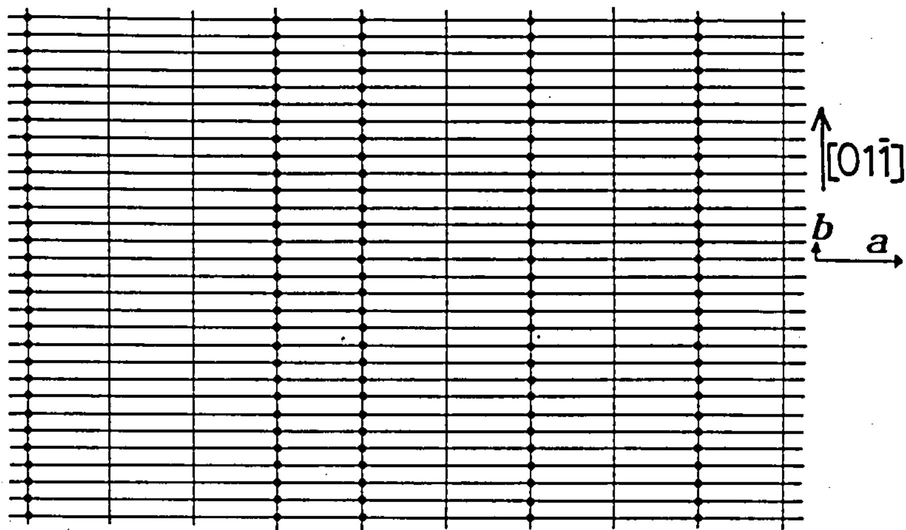

Fig.21 Partially occupied 5x1 surface mesh structure. Solid circles mean that the net points are occupied by surface structures. Length of unit mesh for $[0\bar{1}1]$ is equal to lattice spacing of (100).

$$F = \sum_{m_1} \exp(2\pi i \cdot 500 m_1 p) \sum_{m_2} \exp(2\pi i \cdot 100 m_2 q) \quad . \qquad (6)$$

In this investigation an electron energy for RHEED observation was 80KeV ,and the wavelength of electron beam was 0.042Å and $|\boldsymbol{b}|$(lattice spacing of SiC(011)) was 3.2Å, therefore, the value of λ was decided to be 10^{-2}. Using eq.(6), the scattering intensity is obtained as $F \cdot F^*$. When $r \gg p,q$, the scattering intensity for a small scattering angle is obtained. Figure 22 shows the intensity distribution of the diffracted waves on a screen for the waves perpendicularly incident upon the mesh. In this case, the intensity distribution represents the reciprocal space diagram of the mesh structures. Figure 22(a) shows the diffraction by a fully occupied 5x1 mesh. Peaks correspond to the fifth order streaks observed in the RHEED pattern. The introduction of the parallel rows pointing $\boldsymbol{b}$ shown in Fig.21 results in the increase of the intensity on the lines which are normal to $\boldsymbol{b}$ and connect the peaks as shown in Fig.22(b). Figure 22(b) agreed with the obtained reciprocal space diagram of the surface of 3C-SiC indicated in Fig.20(b). When parallel rows are formed normal to $\boldsymbol{b}$, reciprocal planes are formed normal to $\boldsymbol{a}$ as shown in Fig.22(c). The random missing of mesh points results in the increase of the background intensity as shown in Fig.22(d).

3. Growth on spherically polished Si(111)

In this section, an investigation concerning the introduction of off orientation into (111) substrates is described. Growth was carried out on a spherically polished (111) substrate similar to Si(100). Figure 23(a) shows the surface of a grown layer on the spherically polished substrate. Three narrow black lines spread from the (111) pole to the directions equivalent to $\langle 2\bar{1}\bar{1} \rangle$. Figures 24(a)-(c) show Nomarski microphotographs of the surfaces of the three points on the sample. The positions of the points are schematically indicated in Fig.23(b). The surfaces on the lines are clearly flatter than

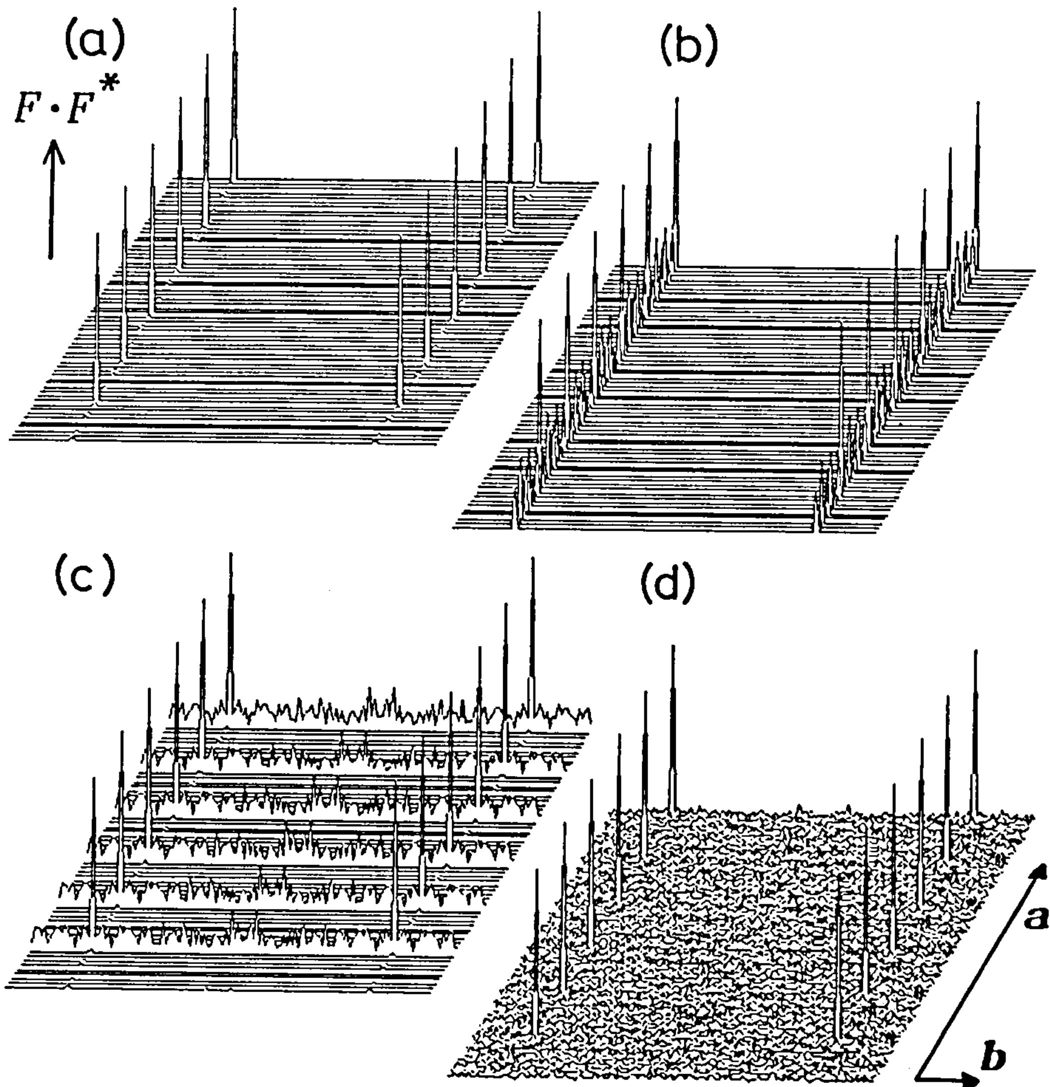

Fig.22 Intensity distribution of diffracted waves on a screen for the incidence azimuth of waves normal to the mesh. (a)Diffraction by fully occupied 5x1 mesh. (b)Diffraction by partially occupied 5x1 mesh which consists of linear arrays pointing to [0$\bar{1}$1]. (c)Diffraction by partially occupied 5x1 mesh which consists of linear arrays pointing to [0$\bar{1}\bar{1}$]. (d)Diffraction by randomly occupied 5x1 mesh.

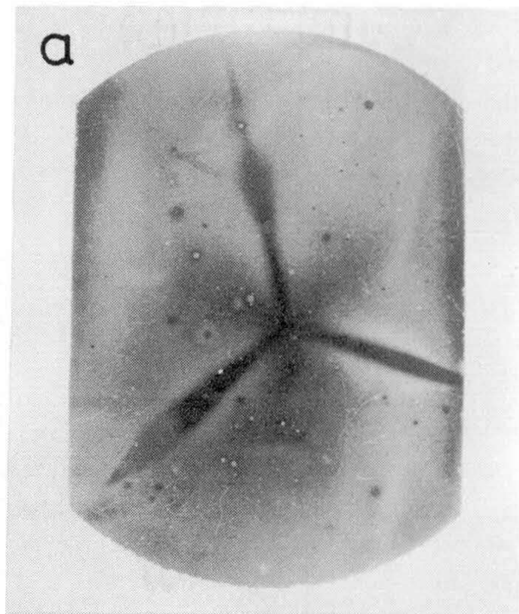

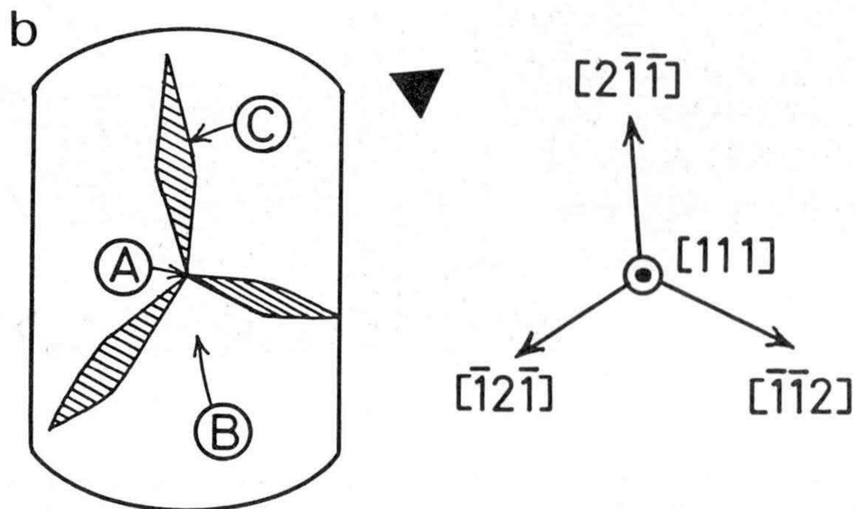

Fig.23 (a)Photograph of the grown layer on a spherically polished (111) substrate. (b)Schematic representation of (a). A solid triangle indicates orientations of etch pits on the Si substrate.

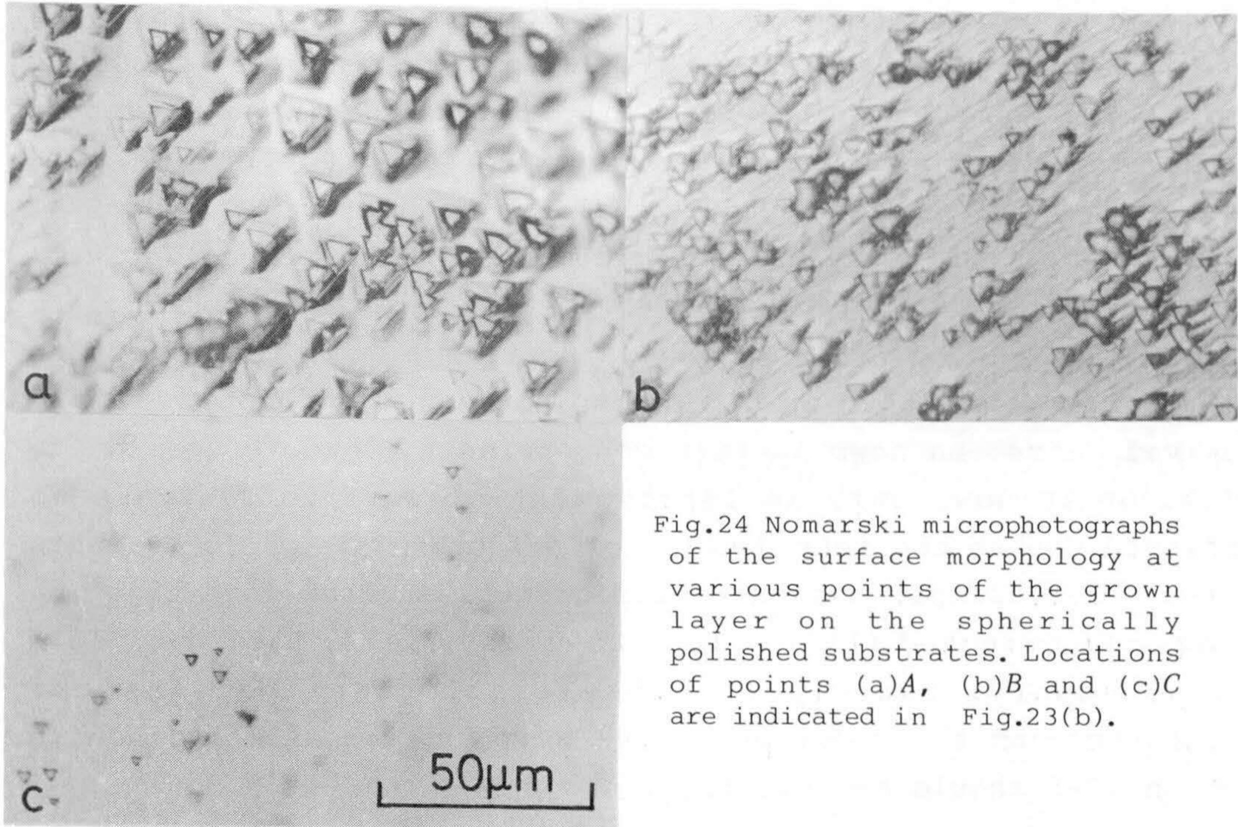

Fig.24 Nomarski microphotographs of the surface morphology at various points of the grown layer on the spherically polished substrates. Locations of points (a)A, (b)B and (c)C are indicated in Fig.23(b).

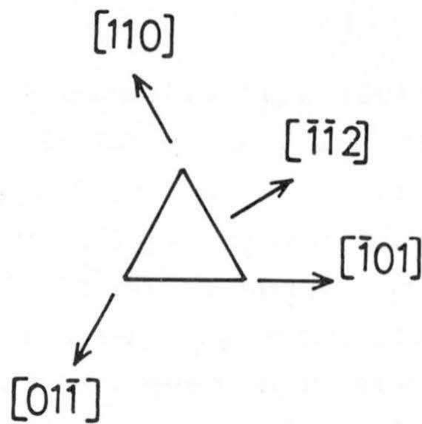

Fig.25 The relationship between orientation and geometry of etch pits on Si(111). (After Runyan, Ref.[21]).

the other part. In the strict sense, $[2\bar{1}\bar{1}]$ is not equivalent to $[\bar{2}11]$ for Si. To distinguish these directions an observation of etch pits was utilized. Pits were formed by boiling spherically polished Si in aqueous KOH at 80°C for 30sec. Triangular pits were formed. The orientation of such pits is known as shown in Fig.25[21]. The directions perpendicular to the three sides of the triangles are $\langle 2\bar{1}\bar{1} \rangle$. The relationship of the orientation between the pits and the three lines are schematically indicated in Fig.23(b). Conclusively, the directions of the off orientation which are effective to improve surface flatness were obtained to be $[\bar{1}\bar{1}2]$, $[\bar{1}2\bar{1}]$ and $[2\bar{1}\bar{1}]$. However, different from the growth on Si(100) the dependence on off orientation was not reproducibly observed. Some unknown factors concerning the growth seemed to exist. Up to now, only an improvement of surface flatness is confirmed due to the introduction of off orientation. To evaluate whether crystallinity was affected or not, further investigation using off oriented (111) wafers towards $[\bar{1}\bar{1}2]$, $[\bar{1}2\bar{1}]$ or $[2\bar{1}\bar{1}]$ are necessary. Especially, the relationship between off orientation and the problems of the warp and cracks mentioned in Section II-5 should be investigated.

4. Summary

Grown layers on (100) well oriented Si substrates contained APD's. As the grown layers became thicker, the area of APD's became broader. However, even for the thick(≃20μm) grown layers they were far from single domain. By the growth on a spherically polished substrate, the introduction of the off orientation to (011) was found to be effective for the elimination of APD's. The elimination of APD's was confirmed for the grown layers on Si wafers oriented 2°, 4° and 6° off (100) towards (011). The domination of steps with bi-atomic layer heights brought about by the introduction of off orientation was considered to be the origin of the elimination of APD's. Molten KOH etching at about 600°C was utilized for the observation of APB's and etch pits.

The identification of the existence of APD's was also possible by the RHEED observation. When the grown layers contained APD's, a mixture of 5x1 and 1x5 surface structures was observed. The surface structure showed extraordinary persistence. The curved and long straight streaks due to reciprocal planes were also observed. Growth on spherically polished Si(111) was also attempted. An improvement in surface flatness by the introduction of the off orientation to $[2\bar{1}\bar{1}]$ was observed.

References

[1] K.Morizane, J. Cryst. Growth 38(1977) 249.

[2] H.Kroemer, K.J.Polasko and S.C.Wright, Appl. Phys. Lett. 36(1980) 763.

[3] B-Y.Tsaur, J.C.C.Fan, G.W.Turner, F.M.Davis and R.P.Gale, Proceeding 16th IEEE Photovoltaic Specialists Conf., San Diego, 1982(IEEE, New York, 1982), p.1143.

[4] M.Akiyama, Y.Kawarada and K.Kaminishi, J. Cryst. Growth 68 (1984) 21.

[5] M.Akiyama, Y.Kawarada and K.Kaminishi, Jpn. J. Appl. Phys. 23(1984) L843.

[6] M.Akiyama, Y.Kawarada and K.Kaminishi, Extended Abstr. 15th Conf. of Solid State Devices and Materials, Tokyo, 1983 (Business Center for Academic Societies Japan, Tokyo, 1983) p.293.

[7] M.Sugo, A.Yamamoto and M.Yamaguchi, Extended Abstr. 33th Spring Meeting of the Japan Society of Applied Physics and of the Related Societies, Tokyo, April, 1986, 4p-W-3.

[8] J.W.Faust,Jr., *Silicon Carbide A High Temperature Semiconductor* (Pergamon Press, Oxford, 1960) edited by J.R.O'Connor and J.Smiltens, p.403.

[9] M.Henzler and J.Clabes, Proceeding 2nd Int. Conf. on Solid State Sufaces, 1974 Jpn. J. Appl. Phys. Suppl. 2, Pt. 2, 1974.

[10] T.Sakamoto and G.Hashiguchi, Jpn. J. Appl. Phys. 25(1986) L78.

[11] R.Kaplan, Surf. Sci. 93, 145(1980).
[12] R.Fischer, H.Morkoc, D.A.Neumann, H.Zabel, C.Choi, N.Otsuka, M.Longerbone and L.P.Erickson, J. Appl. Phys. 60(1986) 1640.
[13] T.Ueda, S.Nishi, Y.Kawarada, M.Akiyama and K.Kaminishi, Jpn. J. Appl. Phys., 25, (1986) L789.
[14] S.L.Wright, H.Kromer and M.Inada, J. Appl. Phys. 55(1984) 2916.
[15] P.N.Uppal and H.Kroemer, J. Appl. Phys. 58(1985) 2195.
[16] M.Tabe, K.Arai and H.Nakamura, Surf. Sci. 99(1980) L403.
[17] H.Lipson and K.E.Singer, J. Phys. C: Solid State Phys. 7(1974) 12.
[18] P.Delescluse and A.Masson, Surf. Sci. 100(1980) 423.
[19] P.J.Dobson, J.H.Neave and B.A.Joyce, Surf. Sci. 119(1982) L339.
[20] C.Kittel, *Introduction to Solid State Physics*, (Wiley, New York, 1986) 6th ed., Chapter 2.
[21] W.R.Runyan, *Semiconductor Measurements and Instrumentation*, (McGraw-Hill, New York, 1975), p.12.